Original Research

Assessment of Infrared Thermography of Thyroid Gland for Development of a New Non-Invasive Sleep Detection System

Farshad Bahramian, Afsaneh Mojra*

Department of Mechanical Engineering, School of Mechanical Engineering, Khajeh Nasir Toosi University of Technology, Tehran, Iran

Received: 05 Nov. 2018   Accepted: 15 Dec. 2018

Abstract

Background and Objective: One of the causes of the human death is the road crashes due to the driver drowsiness or falling asleep. Thermography is one of new techniques for non-invasive automatic detection of driver drowsiness, which could help to prevent sleep-related road accidents. In this research, we aimed to record the temperature of the thyroid gland when a person is awake, drowsy, or starts to fall asleep.

Materials and Methods: For capturing the neck's thermogram, a human thermal video recording was designed. The imaging procedure consisted of the attended cases' preparation, capturing static thermal video of the neck, and analyzing the resultant thermal videos with a particular image-processing algorithm for extracting the temperature data. The image-processing algorithm consisted of image segmentation, noise reduction, and specification of the region of interest for recording the thyroid temperature.

Results: In the wakefulness, a region of the skin, which is in the front of thyroid gland, had an average temperature of 34.5 ± 0.3 °C. A change from being awake to being drowsy and falling asleep reduced the average temperature of the neck area to 33.5 ± 0.2 °C and 32.5 ± 0.1 °C, respectively.

Conclusion: A change from being awake to being drowsy and falling asleep reduces the temperature of the thyroid gland and the neck skin which is located in front of the thyroid gland. By knowing such temperature reduction, a non-invasive system for detection of the person drowsiness or falling asleep can be developed by means of the infrared thermography (IRT).

Keywords: Thermography; Thyroid gland; Sleep

Citation: Bahramian F, Mojra A. **Assessment of Infrared Thermography of Thyroid Gland for Development of a New Non-Invasive Sleep Detection System.** J Sleep Sci 2019; 4(1-2): 9-16.

Introduction

One of the main causes of the car accidents, which results in the death and injury, is driver drowsiness and falling asleep. According to the published statistics by National Highway Traffic Safety Administration (NHTSA) in 2011 and 2013, about 100000 and 72000 road accidents were occurred because of the drivers' drowsiness and falling asleep. Because of these car crashes, about 71000 and 44000 injuries and 1550 and 800 deaths were occurred in 2011 and 2013, respectively (1, 2). There are many assistant systems, which are used for detection of driver drowsiness and falling asleep. These detecting systems are divided into two main categories, invasive and non-invasive. In the invasive methods, by using specific sensors and attaching these sensors to the body of a person, the physiological parameters such as electroencephalogram (EEG) and electrooculography (EOG) are measured and the collected data are used for detection of person drowsiness or falling asleep (3).

Despite a high detection accuracy of these methods, because of sensors attachment to the body organs such as head and causing the discomfort of driver, these methods cannot be used for the detection of driver drowsiness during the driving period (4). Non-invasive methods for detection of the driver drowsiness are divided into two

***Corresponding author**: A. Mojra, Department of Mechanical Engineering, Khajeh Nasir Toosi University of Technology, Tehran, Iran
Tel: +98 21 84063274, Fax: +98 21 88677274
Email: mojra@kntu.ac.ir*

categories. In one of the non-invasive methods, by using specific sensors, car data such as following distance from the front car, number of moves out from the road lane and steering wheel angle are collected during the driving. Collected data are used by the specific algorithms for detection of drowsiness or falling asleep of the car driver. Because of large number of data and long processing time, these methods are less used for the detection of driver drowsiness (4). In the other non-invasive methods, specific cameras and sensors are used for the detection of any unusual state of the driver such as being asleep or drowsy. Data, which are collected from the facial expression of driver, are used by the specific algorithms for analyzing the consciousness of the driver. In these methods, by specific cameras and sensors, driver facial expression such as seating position, head and mouth states, and change of the eye expression are collected. The collected data are then used by the special image processing algorithm for recognition of the level of consciousness of driver (5). Specific sensors, which are used for detection of the driver facial expression and behavior of eyes need suitable amount of ambient light for accurate detection. In these non-invasive methods, parameters such as the skin color of driver, the driving hours, and amount of ambient light affect the detection accuracy of these methods; so, these methods may make mistake in driver sleepiness detection (6).

Previous researches showed that during the sleeping hours, the average body temperature was decreased (7). One of the new imaging techniques, which can be used for measurement of body temperature, is infrared thermography (IRT). Over the last decade, IRT has been widely used for detection of body disorders based on the temperature measurement (8-10). IRT does not emit any harmful rays to the body and collects the IR rays that the body skin emits. This imaging technique is non-invasive and contactless, so the IR camera can be used for detection of the driver drowsiness based on the body parameters such as respiration rate and temperature decrease during falling asleep (11, 12). Ebrahimian Hadi Kiashari et al. (12) conducted a research on the ability of thermal camera for detection of driver drowsiness based on the number of respiration rate and showed that during the sleep, the rate of the respiration decreased in comparison to the normal driver condition. Therefore, by monitoring the driver respiration rate, drowsiness of the driver can be detected. They used thermal camera for monitoring the nostrils area of the driver face and recorded the number of respirations during driving. All of the thermal movies were analyzed by specific image processing algorithm for recording the number of respirations. Pervious researches showed that by using suitable thermal camera for the thyroid gland, the gland could be detected from the neck thermal map (10, 13, 14). This is due to its higher temperature and metabolic activity compared to the surrounding tissue. Because of the location of the thyroid gland and its higher metabolic activity, monitoring and recording the temperature of this gland may be used for driver's drowsiness and sleepiness detection and development of a non-invasive driver's drowsiness detection system.

In this research, thermography technique was used for recording and monitoring the temperature of the thyroid gland when a person is awake, drowsy, and falling asleep. For recording the thyroid gland temperature, a thermography imaging experiment with a particular procedure was designed and neck thermography was done.

Materials and Methods

Study participants: For capturing the thermal movie for recording the temperature of the thyroid gland and neck, thermograms were captured from volunteer subjects. For ensuring of the health state of thyroid of the attended subjects, all of the subjects were asked to have a blood test for measuring thyroid function tests including T3, T3 resin uptake (T3-RU), T4, and thyroid stimulating hormone (TSH) prior the imaging. Then, the subjects with normal thyroid function tests were checked by the endocrinologist for confirmation of a normal thyroid shape and structure. Subsequently, subjects with normal thyroid gland were selected for the neck thermography. The population study consisted of 20 healthy men aged from 24 to 32 years with the average age of 28 years. The average height, weight, and body mass index (BMI) of the study participants were 177 ± 5 cm, 72 ± 10 kg, and 24 ± 3 kg/m^2, respectively.

Neck thermography: For capturing thermogram of the neck and monitoring the temperature of the thyroid gland, when a person is awake, drowsy, and falling asleep, a thermal imaging experiment was designed based on a specific protocol. This thermal imaging procedure consisted of three steps: subjects' preparation, static thermal video capturing, and image processing for recording the temperature of thyroid gland. For preparation of the attended subjects, a specific protocol was used (15). Before imaging, all of the attended subjects were asked to avoid eating meals with caffeine such as tea, coffee, and chocolate 24 hours before imaging. On the imaging day, first, the subject was asked to sit in the imaging room for 10 minutes with uncovered neck and in the position of the imaging, to reach thermal equilibrium with ambient air. After subject's preparation, subjects were informed regarding the experimental procedure based on the Helsinki agreement. At this stage, 5-minute thermal movie was recorded from the subject's neck. The thermal videos were recorded in the thermally-controlled room condition with the air humidity and temperature of 20 ± 5%, and 25 ± 1 °C, respectively. To be ensured of uniform temperature of the test room, several thermometers were used in different locations of the room and air-conditioning system was set up to achieve uniform temperature with minimum gradient all over the room. For capturing thermal video of subjects, FLIR A655sc thermal camera (FLIR Inc, Wilsonville, Oreg, United States of America) was used. This camera has an imaging resolution of 640 × 480 pixels with a maximum accuracy of 0.03 °C and can capture 30 frames per second (FPS) thermal movies (based on the FLIR A655sc user manual). All of the above steps were repeated for recording thermal videos when participants were awake, drowsy, and falling asleep.

Image processing and thyroid temperature extraction: After capturing thermal movie from the subject's neck, the thermal movies were converted to the continuous frames, one frame for each second of the movie. Afterward, image-processing technique with specific steps and algorithms was applied to the entire frames. Image processing stage included segmenting the subjects' neck from the background, reducing the noise, improving the edge of the image boundaries, and extracting and monitoring the temperature of neck skin in front of the approximate location of the thyroid gland.

Segmenting neck from background: In comparison to the ambient temperature of the test room and the background wall, 25 ± 1 °C, body organs such as neck and face, have a higher temperature of about 35 ± 1 °C, because of their higher metabolic activity and heat generation. The higher temperature makes neck and face regions brighter, with high intensity of white color, on the gray-scale thermograms. For segmenting of neck from the background, Bayesian image segmenting technique was used based on different temperature of the subject and background (16). The resultant thermogram after undergoing the Bayesian segmentation algorithm is shown in figure 1a and the pseudo-code of this image-processing step is shown in the figure 1b.

Thermogram noise reduction by anisotropic diffusion filter: Before thermal imaging, all of the ambient factors such as roof lights and air conditioner system, which may make noise in the resultant thermal movie, were set up in a way to produce a minimum noise on the resultant thermal movie. Despite reducing the impact of ambient parameters on the noise of thermal images, the resultant thermograms had little amount of noise which must be removed for accurate data extraction from thermograms. For reducing the noise of thermograms, anisotropic diffusion filter, Perona-Malik, was used (17).

(a)

(b)

```
Bayesian image segmenting
For each pixels (x,y) of subject thermogram
   If temperature of pixel (x,y) ≥ 30 °C
      Pixel (x,y) = 'body part'
   Elseif temperature of pixel (x,y) < 30 °C
      pixel (x,y) = 'backgraound'
   End
End
Segmented thermogram
```

Figure 1. (a) Initial person thermogram extracted from the thermal movie (left), the thermogram after segmenting by Bayesian algorithm (right); (b) Developed pseudo-code for thermogram segmentation

(a)

(b)

Anisotropic diffusion filter noise reduction
Anisotropic diffusion filter (segmented thermogram, 3 step of noise reduction and edge sharpening)
Noise free image with sharp boundaries

Figure 2. (a) Raw thermogram of a person (left), the thermogram after noise reduction by an anisotropic diffusion filter (right); (b) Perona-Malik noise reduction developed pseudo-code

On the captured thermograms, because of heat transfer from the body organs with the higher temperature to their surrounding low-temperature organs, the boundaries of a tissue with higher temperature were not sharp enough and had some kind of blurriness (18). For separating the thyroid gland, which has blurry boundary due to the higher temperature in comparison to its surrounding tissues, first the sharpness of its boundary was increased. This anisotropic diffusion filter had the ability to increase the sharpness of the boundaries and modify the data which existed at these boundaries. The resultant thermogram and the pseudo-code of 3 steps of noise reduction algorithm are depicted in figure 2a and figure 2b, respectively.

Thyroid gland identification: After thermogram segmentation and removing the noise of thermogram, the region of the subject's neck, which is located in the front of the thyroid gland, was chosen by the image-processing algorithm as the region of interest for further analysis. For choosing the neck of the attended subjects, the developed algorithm first used a rectangular region of interest for separating the neck from the rest of the thermogram. Afterward, the central region with the higher temperature and higher intensity of white color in the gray-scale thermogram was chosen as the sign of the thyroid gland. This was because of higher temperature of thyroid gland in comparison to its surrounding areas (10, 13). After specifying the approximate location of the thyroid gland, the average temperature of this area was monitored and recorded during 5-minute recording of the thermal movie while being awake, drowsy, and asleep. Selection of the rectangular region of interest and specifying the approximate location of the thyroid gland are shown in figure 3a. In figure 3b, the real location of the thyroid gland, in blue color, is shown in 3-dimensional and realistic geometrical model of the human neck. The pseudo-code, which is used for this part of algorithm, is depicted in figure 3c.

(a)

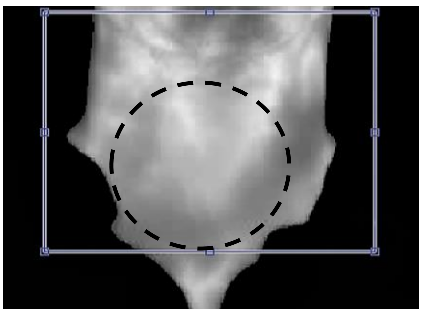

(b)

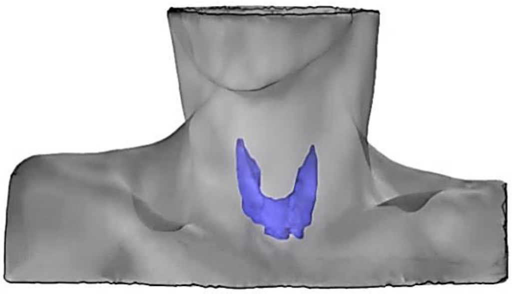

(c)

Specifying the rectangular region of interest and thyroid gland
Rectangle marker (neck of the driver)
Thyroid gland for monitoring and temperature analysis

Figure 3. (a) Location of the thyroid gland, blue tissue at right, the subject's thermogram after choosing the rectangular region of interest and detecting the approximate location of thyroid gland at left; (b) Pseudo-code which is used for this part of image processing

After specifying the approximate location of thyroid gland, every second of thyroid temperature recording was done by the developed algorithm.

P-value less than 0.0500 was considered statistically significant. Statistical analysis was performed by SPSS software (version 25, IBM Corporation, Armonk, NY, USA).

Ethical Approval: All procedures followed were in accordance with the ethical standards of the responsible committee on human experimentation (institutional and national) and with the Helsinki Declaration of 1975, as revised in 2013. Informed consent was obtained from all participants for being included in the study.

Results

For recording the temperature of the thyroid gland, first on the captured neck thermograms, the temperature of thyroid was monitored and recorded. After monitoring, the temperature of thyroid gland for each person in normal condition, tiredness and drowsiness, and sleep were collected. As shown in the figure 4, when the subject was awake, the temperature of the thyroid gland was higher and it was about 34.5 ± 0.3 °C. The temperature of the thyroid gland reduced in the drowsiness and it was about 33.5 ± 0.2 °C, and in the subjects' sleep, it was about 32.5 ± 0.1 °C. The temperature difference between being fully awake, drowsy, and being fully asleep was statistically significant ($P < 0.0001$).

The results of monitoring the temperature of the thyroid gland showed that the metabolic activity and the temperature of this gland were higher when the person was awake. The temperature of the thyroid decreased about 0.5-1 °C and 1.5-2 °C when the person was drowsy and asleep, respectively.

For further analysis, for each subject, the temperature of the thyroid gland was recorded in every second of 5-minute thermal video, every frame of thermal video, and during the capturing of thermal movie. The resultant record of the thyroid gland temperature during the experimental procedure is depicted in figure 5 (a-d) for four of the subjects.

As shown in the figure 5 (a-d), during the normal body activity of a person, the region of the skin located in the front of the thyroid gland had higher temperature than the same area in the same person when the case was drowsy or asleep. The oscillations that exist in the thyroid gland temperature of subjects are due to the excessive heat transfers of the thyroid gland. Thyroid gland in comparison to its surrounding tissues has higher temperature and transfers some of its extra heat to the breathed air for increasing the temperature of breathed air, surrounding tissues, and the ambient air.

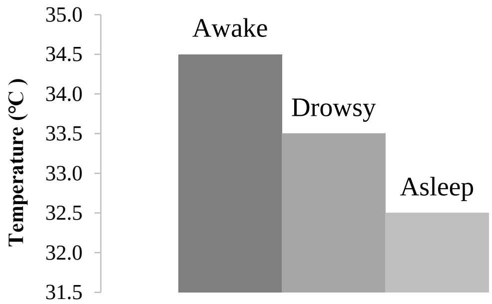

Figure 4. Average temperature of the thyroid gland for all of the attended subjects while being awake, drowsy, and asleep

The neck thermograms of four of the subjects when they were awake, drowsy, and asleep are depicted in figure 6 (a-c). The approximate location of the left and right lobes of the thyroid gland is depicted with black arrows for each subject in figure 6 (a-c).

As depicted in the figure 6 (a-c), during a change from being awake to fully asleep, the temperature of a region of the skin located in front of the thyroid gland decreased about 1.5-2 °C. This decrease of temperature can be used as the sleep biomarker, which can be used for detection of the subject's drowsiness and falling asleep for different applications such as driving or working with instruments which need full consciousness and alertness of the operator.

Discussion

In the present study, the potential of thyroid gland temperature variations as the biomarker of change of a person's consciousness from being awake to being asleep was investigated. For non-invasive temperature measurement, the thermography imaging technique is used for recording the temperature of the thyroid gland from the neck skin while a person is awake, drowsy, and falling asleep.

For capturing the neck thermogram, thermal experiment based on a particular protocol was designed. This standard imaging procedure consists of three main levels of subjects' preparation, capturing static thermal video and image processing, and recording of the temperature of the thyroid gland.

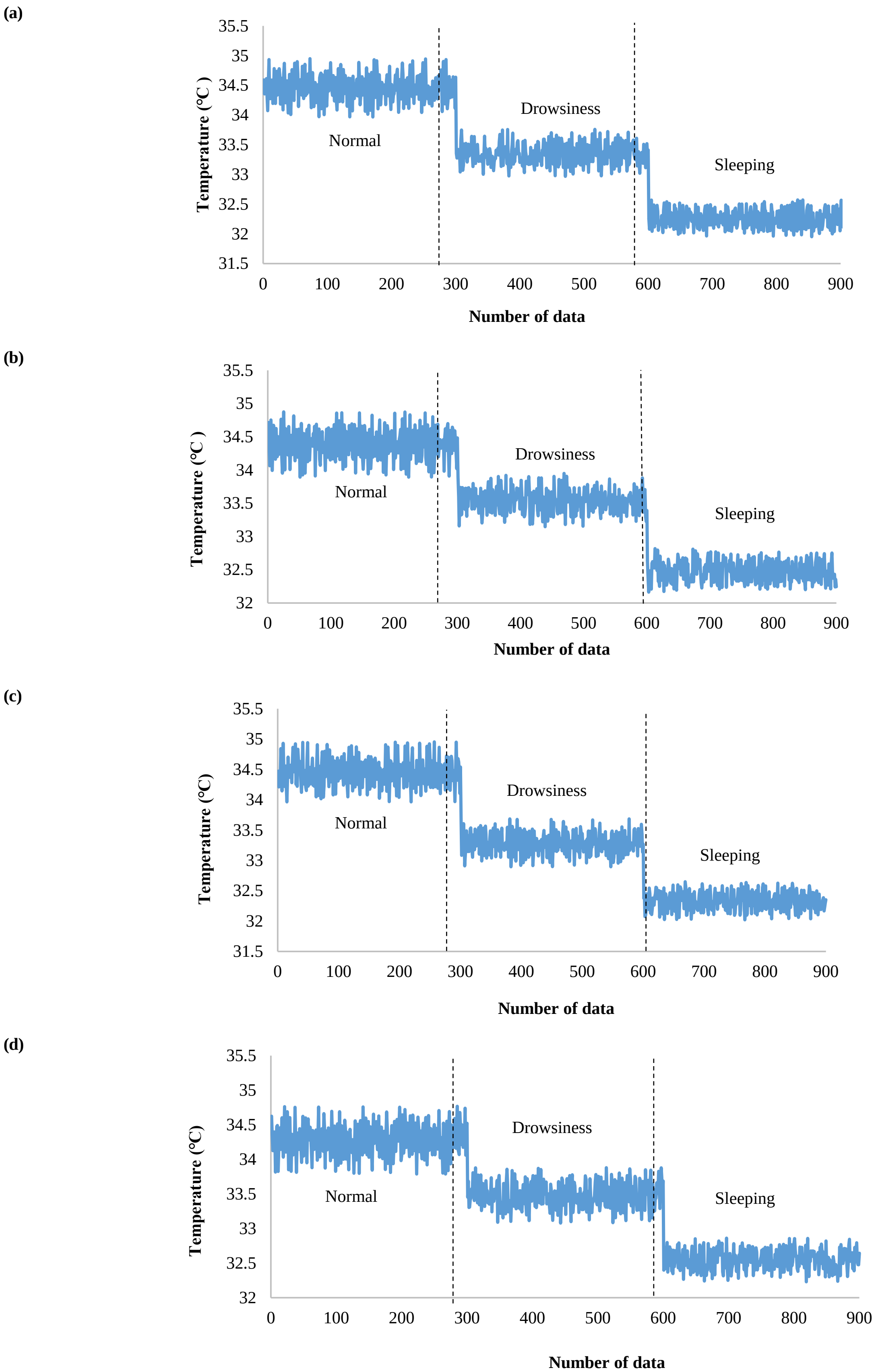

Figure 5. Thyroid gland temperature recording when a person is awake, drowsy, and asleep during the thermal imaging for four of the attended subjects

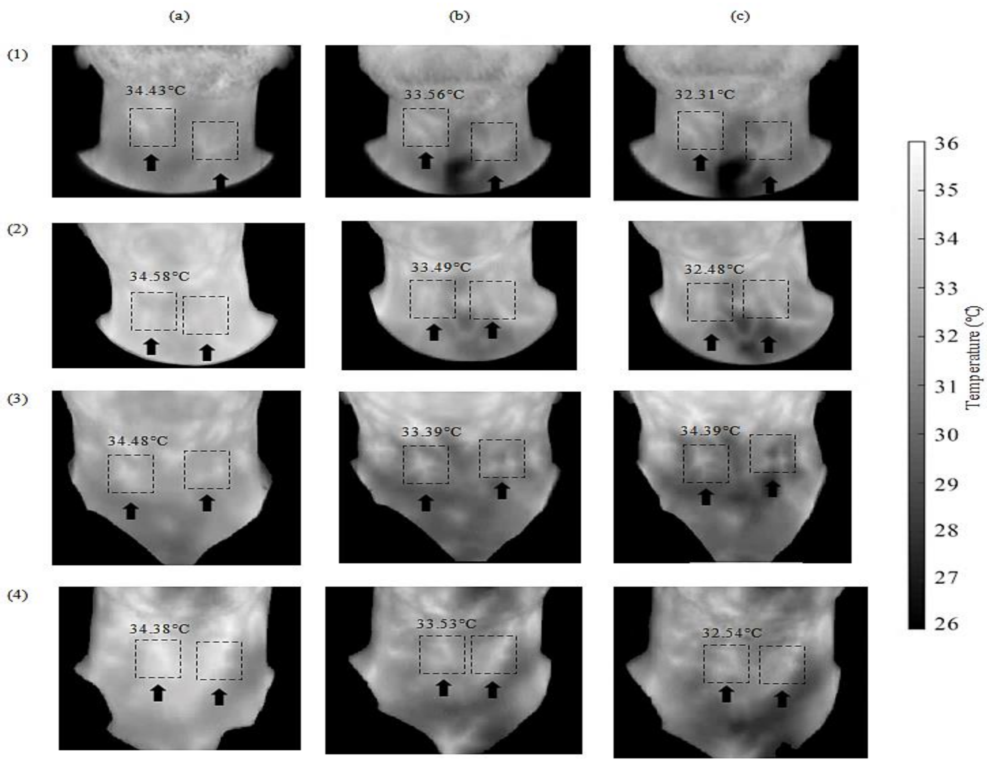

Figure 6. Neck thermograms when being (a) awake, (b) drowsy, (c) asleep, the approximate location of the thyroid gland by the left and the right lobes is shown on the thermograms. Thermograms are presented for 4 sample cases

For the preparation, all of the subjects were asked to avoid eating special meals 24 hours before the examination. On the imaging day, first, all of the subjects rested for a while in the thermally-controlled room with a specified ambient temperature; then, the thermal video with the suitable thermal camera was recorded from the neck of the subjects. After capturing the thermal videos, all of the thermal movies were converted to distinct image frames. All of the resultant frames underwent a particular image-processing algorithm and temperature of the thyroid gland was recorded every second of the 5-minute thermal movie.

The thyroid gland as a heat source produces heat on the neck. Accordingly, the thermogram of the neck includes hot spots in front of the thyroid gland. The hot spots are representative of the left and the right lobes of the thyroid gland. Results of this research reveal that when a person is fully awake and the body has a normal metabolic activity, the thyroid gland has its maximum temperature which is about 34.5 °C. A change from the fully awake condition to the drowsy condition decreases the temperature of the thyroid about 1 °C, and the thyroid has a temperature of 33.5 °C. This temperature reduction could be related to the reduction of the metabolic activity of the body. During falling asleep, the thyroid temperature reaches to its minimum value, which is 32.5 °C. By inspecting the temperature changes of the thyroid gland from being fully alert to the drowsiness and subsequently fully asleep, a non-invasive system for detection of the person drowsiness or falling asleep can be developed by means of the IRT.

Conclusion

Capturing IR thermal images when a person is awake, drowsy, and falling asleep shows that by changing the condition of the human body, temperature of the neck skin, which is located in front of the thyroid gland, has significant variation. The decrease of the thyroid gland temperature with the reduction of the metabolic activity can be used for the drowsiness and sleep detection. Therefore, temperature variation of the thyroid gland could be employed as a biomarker, which makes it appropriate for developing a non-invasive IRT method for drowsiness and sleep detection. This method is applicable to different situations such as driving or working with specific instruments which need complete operator’s consciousness.

Conflict of Interests

Authors have no conflict of interests.

Acknowledgments

This research did not receive any specific grant from funding agencies in the public, commercial, or not-for-profit sectors.

We thank Dr. Ali Nahvi and the Virtual Reality Laboratory at Khajeh Nasir Toosi University of Technology, Teharn, Iran, for assistance with the IR setup and comments that improved the manuscript.

References

1. National Sleep Foundation. National Sleep Foundation White Paper on Drowsy Driving [Online]. [cited 2016 Nov]; Available from: URL: https://drowsydriving.org/2016/11/national-sleep-foundation-white-paper-on-drowsy-driving/
2. National Highway Traffic Safety Administration. NHTSA Drowsy Driving Research and Program Plan [Online]. [cited 2016 Mar]; Available from: URL: https://www.nhtsa.gov/sites/nhtsa.dot.gov/files/drowsy driving_strategicplan_030316.pdf
3. Sahayadhas A, Sundaraj K, Murugappan M. Detecting driver drowsiness based on sensors: A review. Sensors (Basel) 2012; 12: 16937-53.
4. Sigari MH, Fathy M, Soryani M. A driver face monitoring system for fatigue and distraction detection. Int J Veh Technol 2013; 2013: 263983.
5. Khan MI, Mansoor AB. real time eyes tracking and classification for driver fatigue detection. Proceedings of International Conference on Image Analysis and Recognition (ICIAR 2008); 2008 Jun 25-27; Povoa de Varzim, Portugal. Berlin, Germany, Springer: p. 729-38.
6. Ring EFJ. History of thermology and thermography: Pioneers and progress. Thermology international 2012; 22 Appendix: 3-8.
7. Institute of Medicine (US) Committee on Sleep Medicine and Research, Colten HR, Altevogt BM. Sleep disorders and sleep deprivation: An unmet public health problem. Washington, DC: National Academies Press; 2006.
8. Cholewka A, Stanek A, Kwiatek S, et al. Does the temperature gradient correlate with the photodynamic diagnosis parameter numerical colour value (NCV)? Photodiagnosis Photodyn Ther 2013; 10: 33-8.
9. Gonnermann J, Klein JP, Klamann MK, et al. Dry eye symptoms in patients after eyelid reconstruction with full-thickness eyelid defects: Using the Tomey TG-1000 thermographer. Ophthalmic Res 2012; 48: 192-8.
10. Bahramian F, Mojra A. Analysis of thyroid thermographic images for detection of thyroid tumor: An experimental-numerical study. Int J Numer Method Biomed Eng 2019; 35: e3192.
11. Ring F. Thermal imaging today and its relevance to diabetes. J Diabetes Sci Technol 2010; 4: 857-62.
12. Ebrahimian Hadi Kiashari S, Nahvi A, Homayounfard A, et al. Monitoring the variation in driver respiration rate from wakefulness to drowsiness: A non-intrusive method for drowsiness detection using thermal imaging. J Sleep Sci 3:1-9.
13. Jin C, He ZZ, Yang Y, et al. MRI-based three-dimensional thermal physiological characterization of thyroid gland of human body. Med Eng Phys 2014; 36: 16-25.
14. Helmy A, Holdmann M, Rizkalla M. Application of thermography for non-invasive diagnosis of thyroid gland disease. IEEE Trans Biomed Eng 2008; 55: 1168-75.
15. Brioschi ML, Teixeira MJ, Silva FMRM, et al. Medical thermography textbook: Principles and applications. Sao Paulo, Brazil: Andreoli; 2010.
16. Pavlidis I, Tsiamyrtzis P, Manohar C, et al. Biometrics: Face recognition in thermal infrared. In: Bronzino JD, editor. Biomedical engineering handbook. Boca Raton, FL: CRC Press; 2006.
17. Perona P, Malik J. Scale-space and edge detection using anisotropic diffusion. IEEE Trans Pattern Anal Mach Intell 1990; 12: 629-39.
18. Garbey M, Merla A, Pavlidis I. Estimation of blood flow speed and vessel location from thermal video. Proceedings of the 2004 IEEE Computer Society Conference on Computer Vision and Pattern Recognition, 2004 (CVPR 2004); 2004 27 Jun-2 Jul; Washington, DC, USA.